General Disclaimer

One or more of the Following Statements may affect this Document

- This document has been reproduced from the best copy furnished by the organizational source. It is being released in the interest of making available as much information as possible.

- This document may contain data, which exceeds the sheet parameters. It was furnished in this condition by the organizational source and is the best copy available.

- This document may contain tone-on-tone or color graphs, charts and/or pictures, which have been reproduced in black and white.

- This document is paginated as submitted by the original source.

- Portions of this document are not fully legible due to the historical nature of some of the material. However, it is the best reproduction available from the original submission.

X-622-69-210
PREPRINT

NASA TM X-63576

AN OZONE MEASUREMENT IN THE MESOSPHERE AND STRATOSPHERE BY MEANS OF A ROCKET SONDE

ERNEST HILSENRATH
LESTER SEIDEN
PHILIP GOODMAN

MAY 1969

GSFC

GODDARD SPACE FLIGHT CENTER
GREENBELT, MARYLAND

AN OZONE MEASUREMENT IN THE MESOSPHERE

AND

STRATOSPHERE BY MEANS OF A ROCKET SONDE

by

Ernest Hilsenrath
Goddard Space Flight Center
Greenbelt, Maryland 20771

Lester Seiden* and Philip Goodman
Panametrics, Inc.
Waltham, Mass. 02154

*Present address: General American Transportation Company, Chicago, Ill.

ABSTRACT

A measurement of the ozone content of the mesosphere and stratosphere was performed at Wallops Island, Virginia, on 16 September 1968, using a newly developed parachute sonde released from a rocket. The sonde determines ozone mixing ratio, in situ, as a function of altitude by means of a sensor containing a chemiluminescent detector. The atmosphere is sampled by self pumping as the sonde descends on a specially designed high-altitude parachute. Calibration of the ozone sensor is accomplished immediately prior to flight by sampling known concentrations of ozone at rates expected during a flight. An ozone profile of approximately 2-km resolution was obtained from 67 km to 18 km. A small secondary peak was measured at approximately 62 km. An ozone mixing-ratio maximum of 16 μgram/gram was measured at 34 km and a concentration peak of 5×10^{12} molecules/cm^3 was measured at 25 km. The estimated error in the measurement between 57 km and 20 km is about ±20%, and about ±50% at the other altitudes. The chemiluminescent sonde-measured profile agrees well with other rocket and balloon observations flown simultaneously with this flight in the altitude regions where the measurements overlap.

TABLE OF CONTENTS

LIST OF ILLUSTRATIONS

TABLE

AN OZONE MEASUREMENT IN THE STRATOSPHERE AND MESOSPHERE BY MEANS OF A ROCKET SONDE

Introduction

In the lower stratosphere, the ozone content is a quasiconservative property of the atmosphere and hence can be used in various meteorological studies concerning the scales of atmospheric motions. At higher levels, because of the strong absorption of solar ultraviolet radiation by ozone, this atmospheric constituent plays a dominant part in the earth's radiative-thermal budget. Thus ozone measurements in the stratosphere and lower mesosphere can yield valuable information with regard to atmospheric structure and dynamics, including effects due to the absorption and emission of radiation and the interacting chemical processes.

At the present time, ozone soundings are carried out routinely via balloon ozone sondes at altitudes of up to about 30 km [Hering, 1966; Komhyr et al., 1968]. Total ozone measurements are conducted from ground-based stations throughout the world in cooperation with the World Meteorological Organization. Recently, a few rocket measurements have been made both here and abroad, using optical and chemical techniques [Krueger and McBride, 1968; Randhawa, 1967; Bancarel and Vassey, 1966].

The chemiluminescent ozone sonde described in this paper allows day or night ozone measurements from about 65 km to about 20 km. The measurements may be performed at locations where knowledge of the ozone content has significant geophysical implications, such as the polar regions during winter and the equatorial regions at the equinoxes.

Theory of Operation of Ozone Sensor

The ozone sensor uses the chemiluminescent principle first discussed by Beranose and Rene [1959]. A rocket-borne sonde based on a similar principle has been developed by Randhawa [1967], however, significant differences exist between the sonde described in this paper and that of Randhawa in regard to calibration, chemiluminescent material, and flow-rate measurement. Numerous laboratory studies have been performed to establish the validity of the present method and to verify the assumptions upon which it is based. These studies have confirmed that under flight conditions the sonde will not be affected by atomic oxygen.

Exposure of the chemiluminescent material to ozone causes luminescence which is proportional to the ozone flux. This relationship is expressed by

$$L \propto [0_3] \times \text{flow rate} \qquad (1)$$

where L is the light intensity, and $[0_3]$ is the ozone concentration. The linear dependence upon ozone flux has been amply demonstrated in the laboratory over the range of flow rates encountered by the ozone sensor in a parachute descent from approximately 65 km to 20 km.

In flight, air is sampled by the sensor by means of a self pumping mechanism, depicted in Figure 1. The ballast chamber is connected to the ambient atmosphere through an inlet pipe and is initially in pressure equilibrium with the atmosphere. When the sensor is released at apogee and descends through the atmosphere on the parachute, the pressure inside the ballast chamber will tend to equilibrate with the increasing external pressure, resulting in a net flow of gas through the inlet pipe. The detector, consisting of the chemiluminescent material and the photometer,

is positioned along the inlet pipe and is thus continuously exposed to the ambient atmosphere.

An expression for flow rate of air into the ballast chamber can be derived from the equation of state for an ideal gas, $PV = nRT$:

$$\frac{dn_b}{dt} = \frac{d}{dt}\left(\frac{P_b V_b}{RT_b}\right) = \frac{V_b}{R}\left[\frac{1}{T_b}\frac{dP_b}{dt} - \frac{P_b}{T_b^2}\frac{dT_b}{dt}\right]$$
$$= \frac{V_b}{RT_b}\left[\frac{dP_b}{dt} - P_b\frac{d(\ln T_b)}{dt}\right] \qquad (2)$$

n_b = number of moles of air in ballast chamber

P_b = pressure in ballast chamber

V_b = volume of ballast chamber

R = Universal gas constant

T_b = temperature in ballast chamber

The mass flow rate into the ballast chamber is then given by

$$\frac{dm}{dt} = M\frac{dn_b}{dt} = \frac{MV_b}{RT_b}\left[\frac{dP_b}{dt} - P_b\frac{d(\ln T_b)}{dt}\right] \qquad (3)$$

where

m = mass of air in ballast chamber

M = molecular weight of air = 28.96

It is important to note that P_b and T_b in equations 2 and 3 refer to conditions inside the ballast chamber, not the ambient environment.

Equation 1 can be written as

$$L = K \frac{m(0_3)}{m(air)} \frac{dm_b}{dt} = KQ \frac{dm_b}{dt} \tag{4}$$

where

K = proportionality factor, including sensitivity of the detector

$Q = m(0_3)/m(air)$ = mass-mixing ratio of ozone to air

Substitution of equation 3 into equation 4 yields

$$L = KQ \frac{MV_b}{RT_b} \left[\frac{dP_b}{dt} - P_b \frac{d(\ln T_b)}{dt} \right] \tag{5}$$

Since T_b is nearly constant during a flight, and is measured, it is convenient to write equation 5, to a first approximation, as:

$$L = K'Q \frac{dP_b}{dt} \tag{6}$$

where $K' = K M V_b/R T_b$ is regarded as constant. This equation simply states that the luminescence is proportional to the ozone mixing ratio times the rate of change of pressure in the ballast chamber.

Description of Ozone Sonde

The ozone sensor is depicted in Figure 2 and its block diagram is shown in Figure 3. Ambient air enters the inlet port and flows past a light baffle that excludes external light from the photometer. The inlet tube conductance for air-flow is high, the pressure time constant of the system being less than one second. The incoming air is sampled for ozone content by the chemiluminescent detector, which is composed of rhodamine-B dye absorbed on a porous Vycor substrate [NASA Tech. Brief, 1965; Seiden, 1966]. The luminescence produced is monitored by a photomultiplier with an S-20 response, a light

chopper, and an A.C. amplifier. A small reference lamp near the photomultiplier provides a calibration signal every 40 seconds. Two diaphragm-type pressure transducers whose ranges are 0 to 5 Torr and 0 to 100 Torr are connected to the ballast chamber. The output of the 0 to 5 Torr (1 volt/Torr) transducer is electronically processed in flight to yield dP/dt directly. A thermistor is mounted on the ballast-chamber housing to indicate the temperature. A high voltage reference signal is also provided to monitor the photomultiplier high voltage power supply. The sensor outputs are telemetered to the ground by an in-flight calibrated FM/FM telemetry system.

Two magnetometers (not shown) provide the sonde attitude during descent to permit evaluation of the aerodynamic effects on the selfpumping mechanism. For example, it was observed that severe oscillations in the sonde attitude can be correlated with similar oscillations in the sensor data, which for the flight reported are responsible for the larger measurement uncertainty assigned to the higher altitude data.

The payload parameters are summarized in Table 1. The payload assembly is shown in Figure 4, and the flight deployment sequence in Figure 5.

Table 1

Vehicle and Payload Parameters

Vehicle	Nike-Cajun
Payload weight	200 lb
Payload length	107 in.
Sonde weight	35 lb
Parachute	48 ft Disc-Gap-Band (Murrow et al., 1966)

Calibration

Preflight sensor calibration is performed by exposing the instrument to an air stream of known concentrations of ozone at known flow rates. Though earlier laboratory experience has demonstrated the linear dependence of the luminescence on ozone flux, it is desirable to simulate flow rates, pressures, and ozone quantities expected during an actual flight. From the descent rate of the parachute, dh_f/dt, and from the hydrostatic equation, $dP/dh = -\rho(h)g$, the rate-of-change of the ambient pressure, P_f, encountered during descent, can be written as

$$\frac{dP_f}{dt} = -\rho(h)g\,\frac{dh_f}{dt} \qquad (7)$$

The profiles of P_f and dP_f/dt with time, using the U.S. Standard Atmosphere, are shown in Figures 6 and 7 respectively. A good approximation of dP_f/dt, as given by equation 7, is accomplished by the ozone calibrator shown in Figure 8. The calibrator and sensor are first preconditioned by extensive exposure to high ozone concentrations, to remove ozone-destroying materials. This is a very critical step in the calibration procedure if low ozone concentrations are to be measured. The calibrator and sensor pressure is then reduced to less than 0.1 Torr (corresponding to 70 km altitude), and the pump is valved off. Dried air at atmospheric pressure is moved past the ozone generator, a small mercury lamp; and the air, plus ozone, is allowed to enter the low pressure region of the calibrator through the needle valve, L_1. At this point the air is sampled for ozone content by a Mast-Brewer electrochemical ozone meter [Brewer and Milford, 1960]. The calibration begins

when L_1 is opened and the volumes V_1 and V_2 fill with air plus ozone via the calibrated leaks, the ozone mixing ratio remaining constant throughout the calibration process. The volumes V_1 and V_2 and the leaks L_1 and L_2 are chosen so that the pressure rise in V_2 matches dP_f/dt in equation 7 [Seiden, 1966]. The pressure rise in the ozone sensor ballast chamber and the photometer responses are monitored during the calibration, which lasts approximately 10 minutes. This operation simulates the pressure profile encountered in a parachute drop from approximately 70 km to approximately 30 km. The slope of a plot of the observed luminescence vs dP_f/dt at a fixed ozone mixing ratio yields the calibration constant of the ozone sensor, by equation 6.

The Flight

On September 16, 1968 at 1:00 p.m., EST, a chemiluminescent ozone sonde was launched from Wallops Island, Virginia. (Two sondes were also flown at Point Barrow, Alaska, 71° N, in January 1969. This data will be reported at a later date.) An ozone profile was obtained despite a partial parachute failure which resulted in a descent rate approximately twice that expected. A Naval Weapons Center optical rocket ozone sonde (ROCOZ) of the type described by Krueger and McBride [1968], and electrochemical ozone balloon sondes of the Air Force Cambridge Research Laboratory Mast-Brewer type [Hering, 1966] and the Environmental Science Services Administration type [Komhyr et al., 1964] were flown in support of this flight. A Dobson total ozone measurement was also performed at the ESSA station at Wallops Island in conjunction with the balloon flights. A rocket grenade experiment

[Nordberg et al., 1964] and two meteorological arcasondes were also flown for meteorological support data.

Results

Figure 9 shows the results of this flight. Note the mixing ratio maximum of the 16 μgram/gram at 34 km, whereas balloon data have generally indicated a constant mixing ratio above 30 km, and the small secondary peak at about 62 km. Since the measurement yields ozone mixing ratio by equation 6, rather than ozone density, it is necessary to determine the ambient air density independently. The air density data used to calculate the ozone density were obtained from both the rocket grenade experiment and the two meteorological arcasondes. The resulting ozone-number density profile is shown in Figure 10, indicating excellent agreement with the ROCOZ flight (details of which are to be published independently by A. J. Krueger) and the ESSA and AFCRL balloon sondes. The agreement between the balloon sondes and the chemiluminescent rocket sonde above the ozone peak is also very good. The somewhat poorer agreement below 20 km is attributed to inaccuracies in the flow rate measurement of the chemiluminescent sonde, and to a small amount of residual glow of the chemiluminescent material.

In regard to the data above 57 km, the comparison with the airglow measurement performed in 1960 at night [Reed, 1968] is for illustrative purposes only. Chemiluminescent sonde data quality was considerably degraded because of excessive sonde oscillations in this altitude region due to the partial deployment of the parachute as mentioned above. High altitude resolution was also lost because

of the rapid descent rate, and thus, measurement of fine structure in the ozone profile, if any, was not possible. Altitude resolution was approximately 2 to 3 km above 57 km and a little greater than 1 km below this region. The estimated error of the mixing ratio data is ±20% between 57 km and 20 km and about ±50% outside this region, including a ±5% error associated with the electrochemical ozone meter used in the sensor calibration. Error bars are shown as horizontal lines in Figure 9 and are directly transferred to Figure 10, that is, no additional errors were assigned to the air density measurements.

Although the data shown in Figure 10 generally agree with Reed's nighttime measurement in indicating a secondary peak at 60 km, these data, because of the large uncertainty of the measurement in this region, should not be construed as supporting the existence of a secondary peak in the daytime. However, such a peak or inflection in the ozone profile has been calculated by London [1966] for a simple oxygen atmosphere in photochemical equilibrium in the summer at 15° latitude. Within the indicated error, the data presented here are also in agreement with the ozone profile calculated by Hunt [1966] for a nonequilibrium moist atmosphere at noon in the 35 km to 60 km region. On the other hand, Weeks and Smith [1968] have recently reported optical measurements of ozone which included results for altitudes between 59 km and 65 km that are lower by a factor of four than our data.

Summary and Conclusions

The success of this flight not only demonstrates the validity of the calibration, in that the chemiluminescent detector displayed excellent stability with respect to ozone sensitivity, but also the large altitude range that can be covered by the chemiluminescent ozone sonde. Because of this versatility, ozone measurements can be performed at various latitudes and seasons, day or night, during the significant geophysical events such as the D-region anomaly, the solar eclipse, and the breakdown of the winter polar stratospheric circulation vortex.

REFERENCES

Bancarel, J. P., and A. Vassey, Repartition Verticale de l'Ozone Obtenue en Fusee, Acad. Sci. (Paris) Comptes Rendus, 263 (Serie B), 845-847, 1966.

Beranose, H. J., and M. G. Rene, Oxyluminescence of a Few Fluorescent Compounds of Ozone, Ozone Chemistry and Technology, Advances in Chemistry Series, 21, 7-12, 1959.

Brewer, A. W., and J. R. Milford, The Oxford-Kew Ozone Sonde, Proceedings of the Royal Society, 256, 470-495, 1960.

Hering, W. S., Ozone and Atmospheric Transport Processes, Tellus, 18(2), 470-495, 1966.

Hunt, B. G., Photochemistry of Ozone in a Moist Atmosphere, Journal of Geophysical Research, 71(5), 1385-1398, 1966.

Komyhr, W. D., R. D. Grass, and R. A. Proulx, Ozonesonde Intercomparison Tests, ESSA Technical Report ERL 85-APCL 4, 1968.

Krueger, A. J., and W. R. McBride, Sounding Rocket - OGO IV Satellite Experiments: Rocket Ozonesonde Measurement, Naval Weapons Center TP 4667, December 1968 (available through DDC).

London, J., The Average Distribution and Time Variation of Ozone in the Stratosphere and Mesosphere, Space Research VII, North-Holland Publishing Company, Amsterdam, 175-185, 1966.

Murrow, H. W., and C. V. Eckstrom, Description of a New Parachute Designed for Use with Meteorological Rockets, AIAA Paper 63-699, 1966.

NASA Technical Brief 65-10364, 1965.

Nordberg, W., and W. Smith, Rocket Grenade Experiment, NASA Technical Note TND-2107, 1964.

REFERENCES (Continued)

Randhawa, J., Ozone Sonde for Rocket Flight, Nature, 213, 53-54, 1967.

Reed, E. J., A Night Measurement of Mesospheric Ozone by Observation of Ultraviolet Airglow, Journal of Geophysical Research, 73, 2951-2957, 1968.

Seiden, L., Development of a Chemiluminescent Drop Sonde, NASA Contractor Report CR# 87984 (STAR # N67-36042), 1966 (available through clearinghouse for Federal Scientific and Technical Information, Springfield, Va. 22151).

Weeks, L. H., and L. G. Smith, A Rocket Measurement of Ozone Near Sunrise, Planet. Space Sci., 16, 1189-1195, 1968.

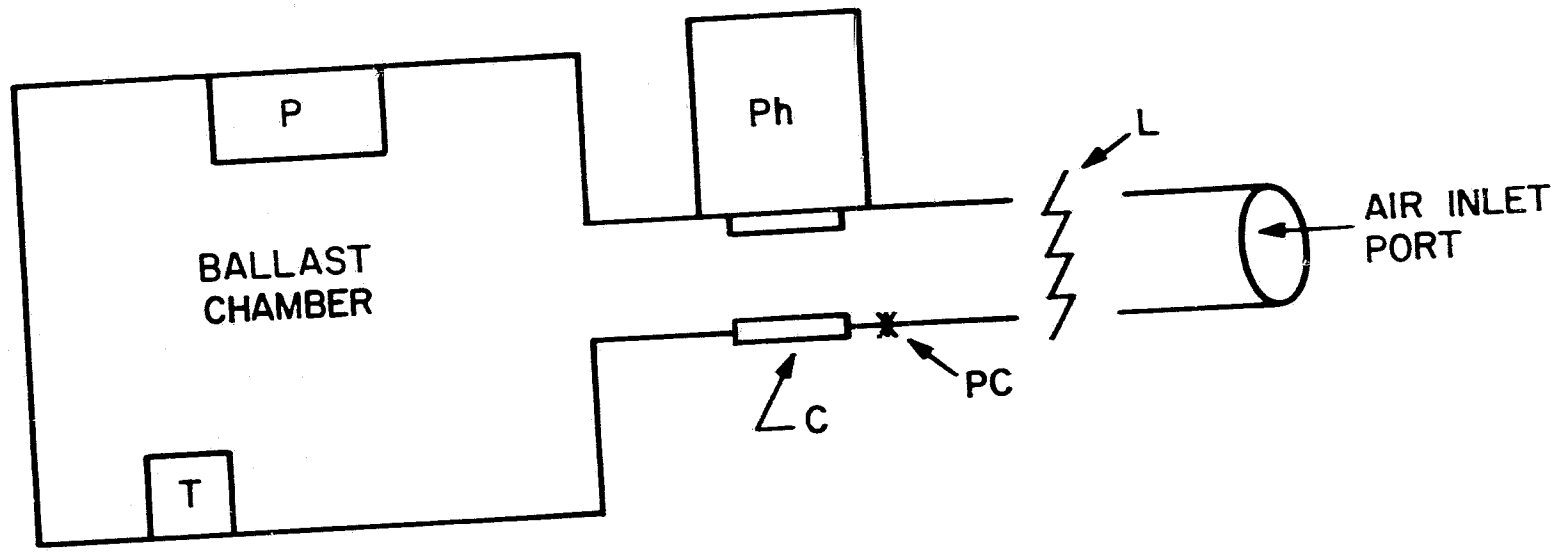

C — CHEMILUMINESCENT DETECTOR
L — LIGHT BAFFLE
P — PRESSURE TRANSDUCER
Ph — PHOTOMETER
PC — PHOTOMETER CALIBRATION SOURCE
T — TEMPERATURE GAUGE

Figure 1. Ozone sensor schematic diagram.

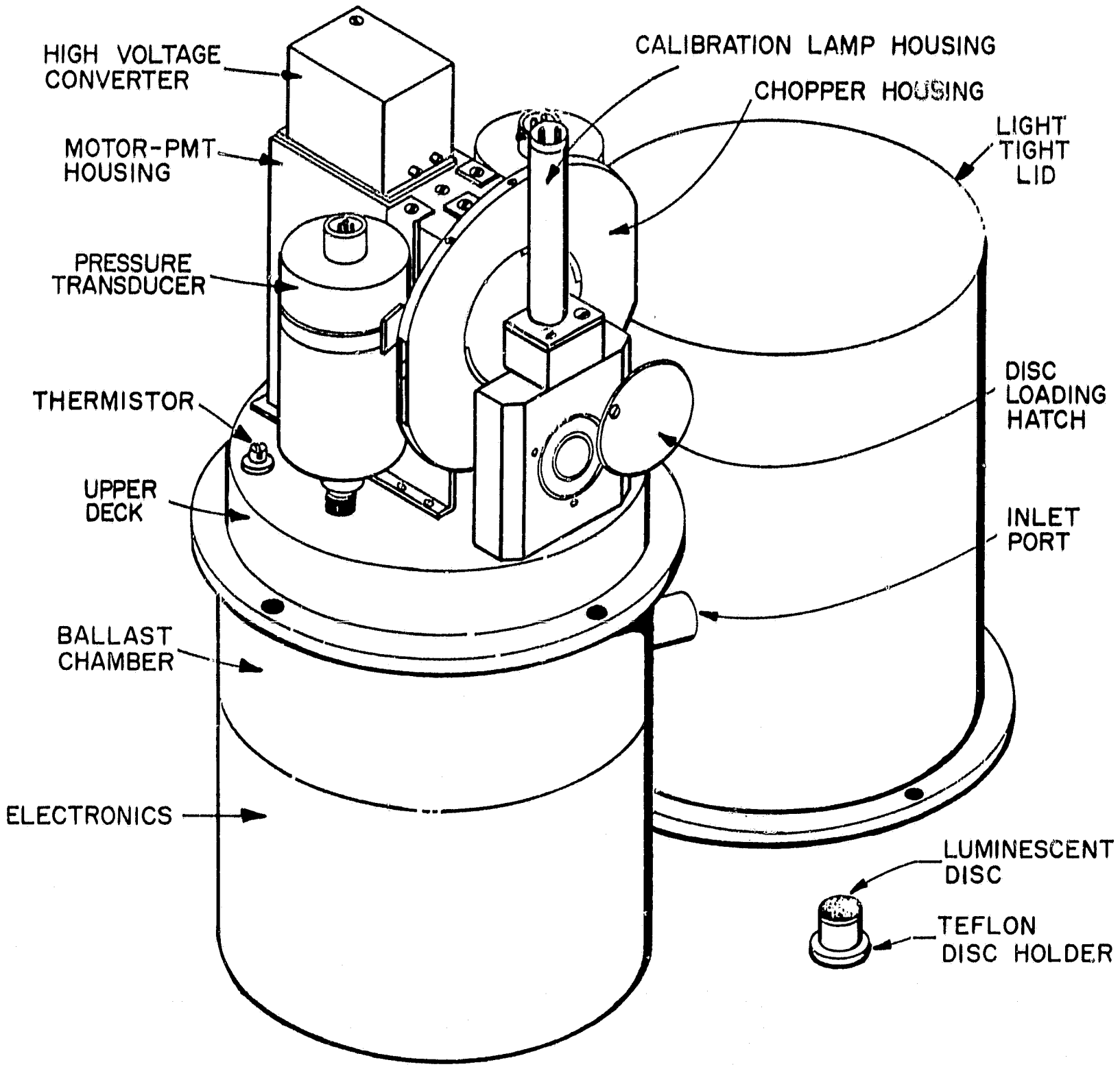

Figure 2. Ozone sensor flight unit.

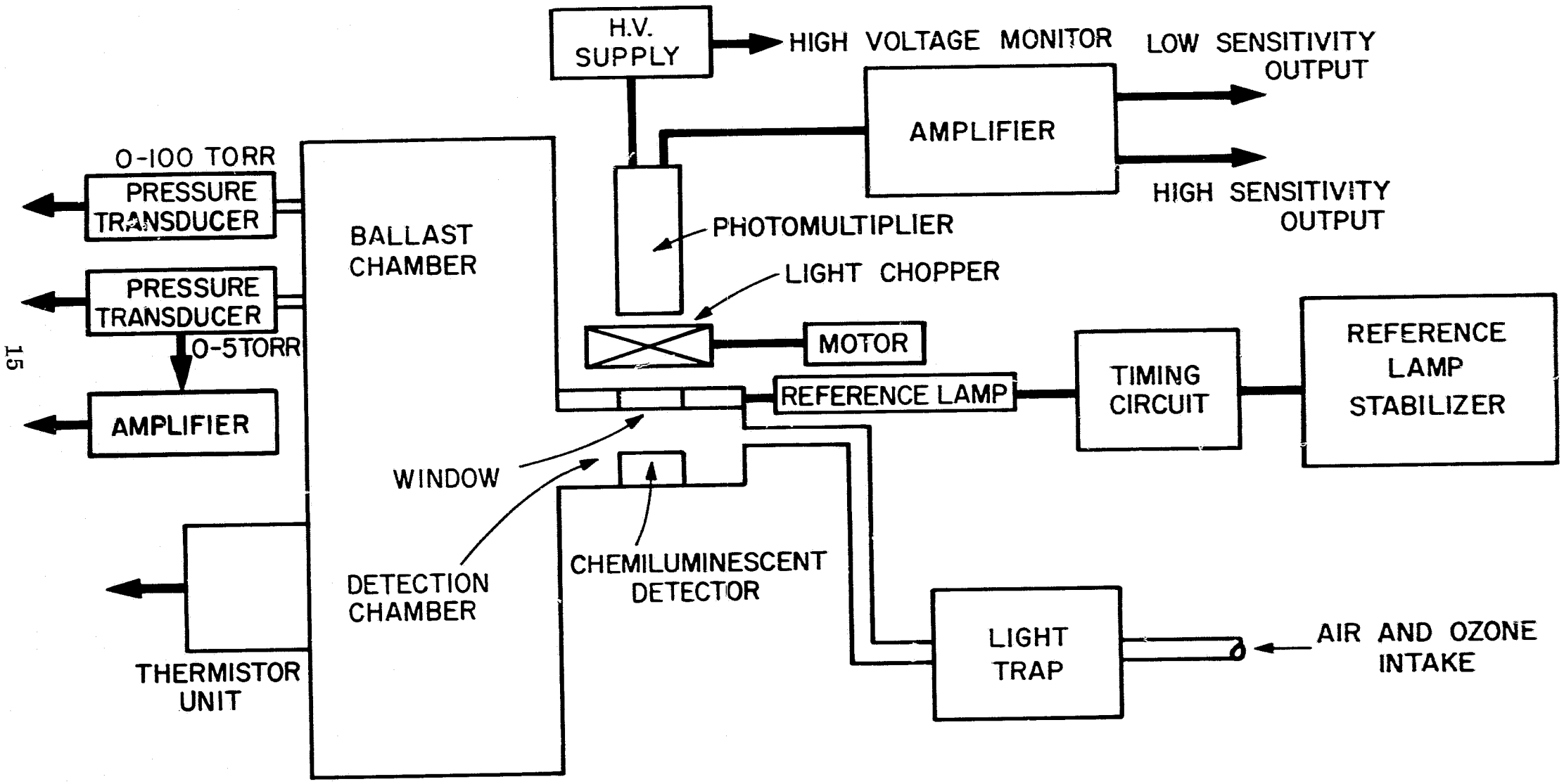

Figure 3. Ozone sensor block diagram.

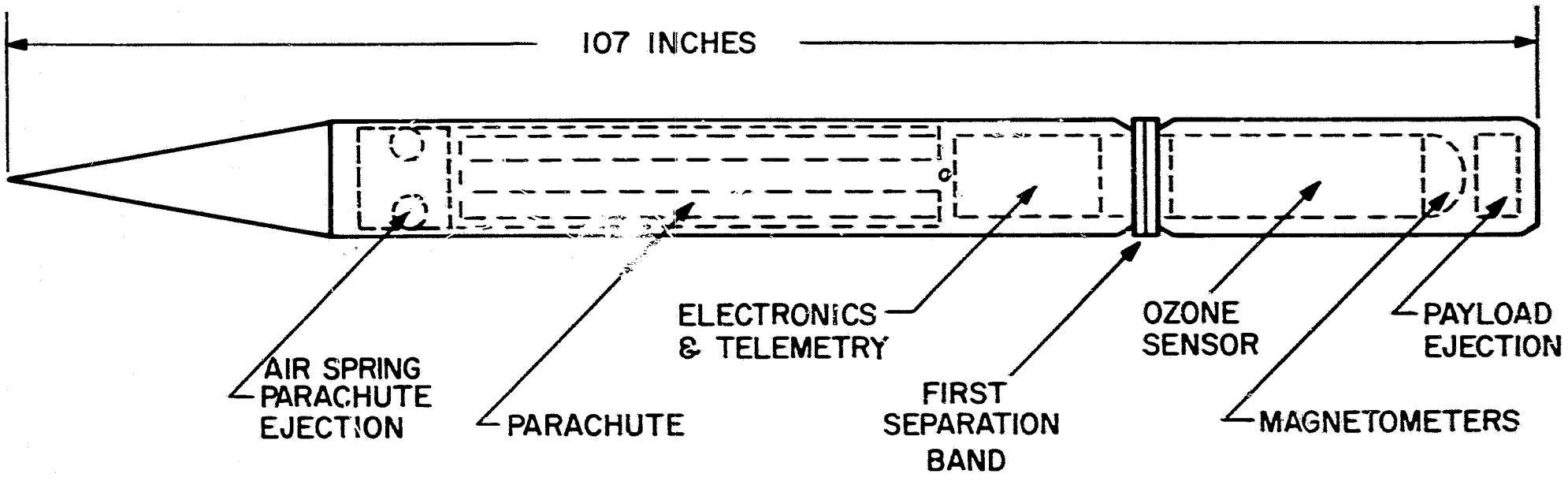

Figure 4. Payload assembly.

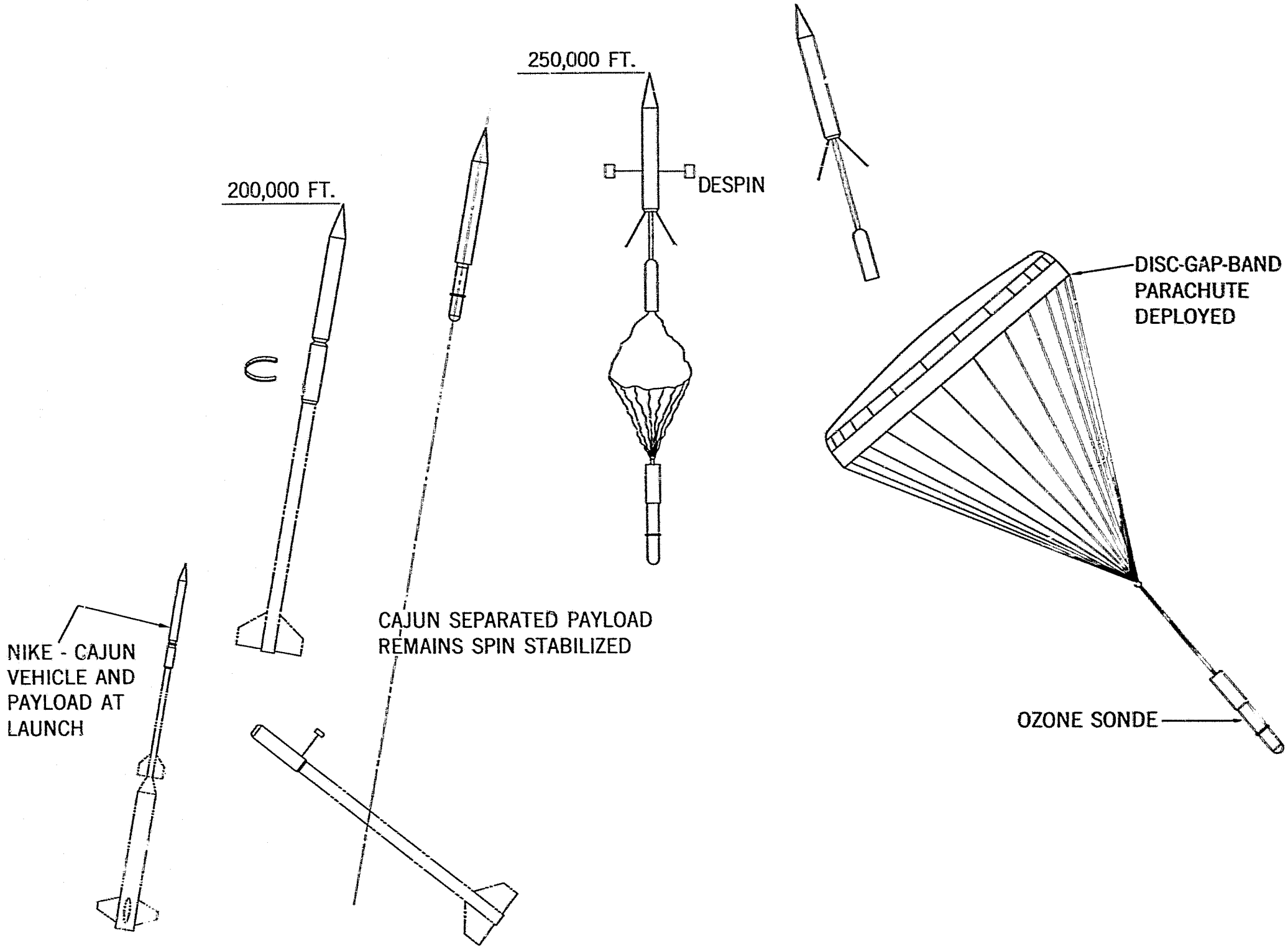

Figure 5. Flight sequence of events.

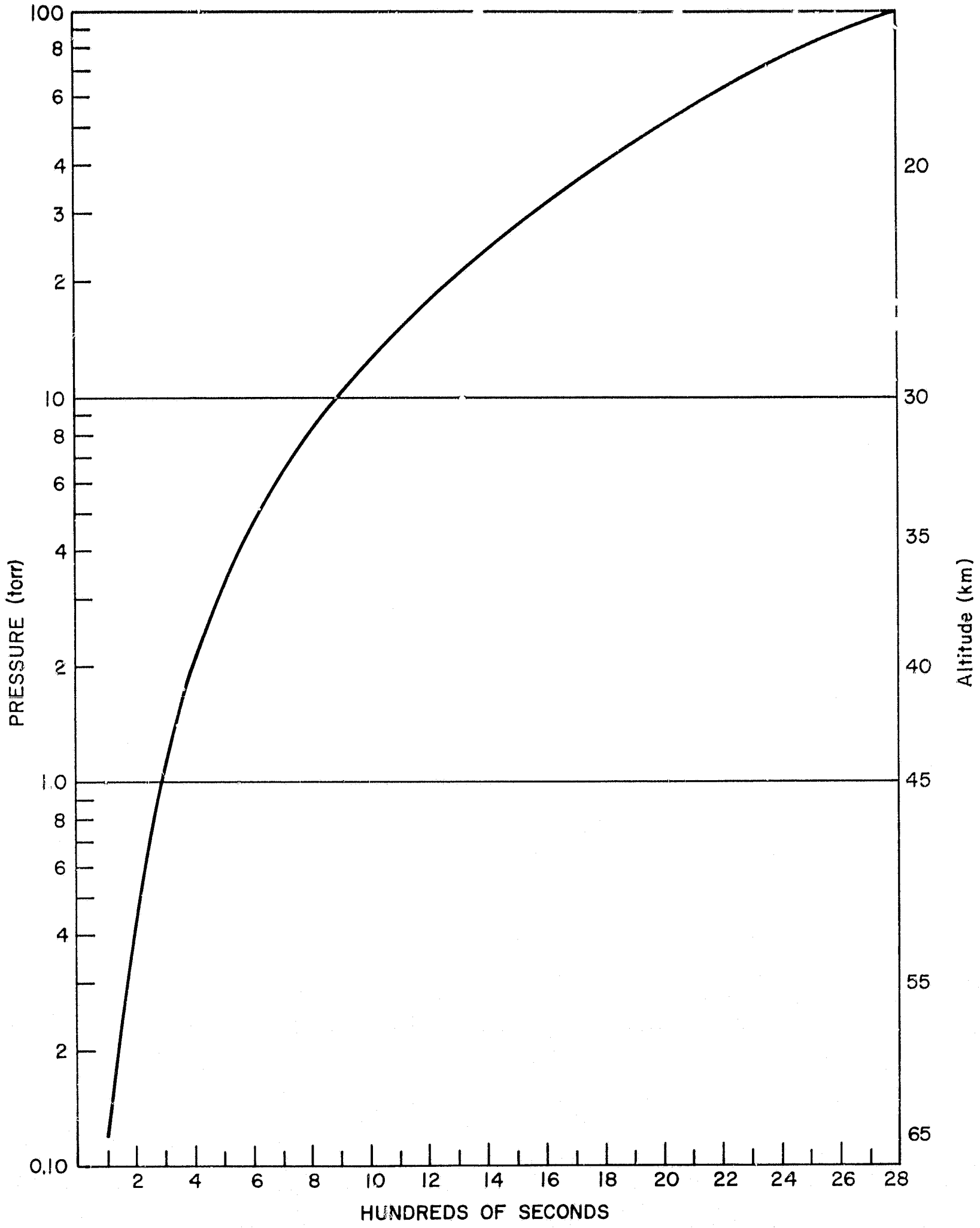

Figure 6. Expected ambient pressure vs descent time.

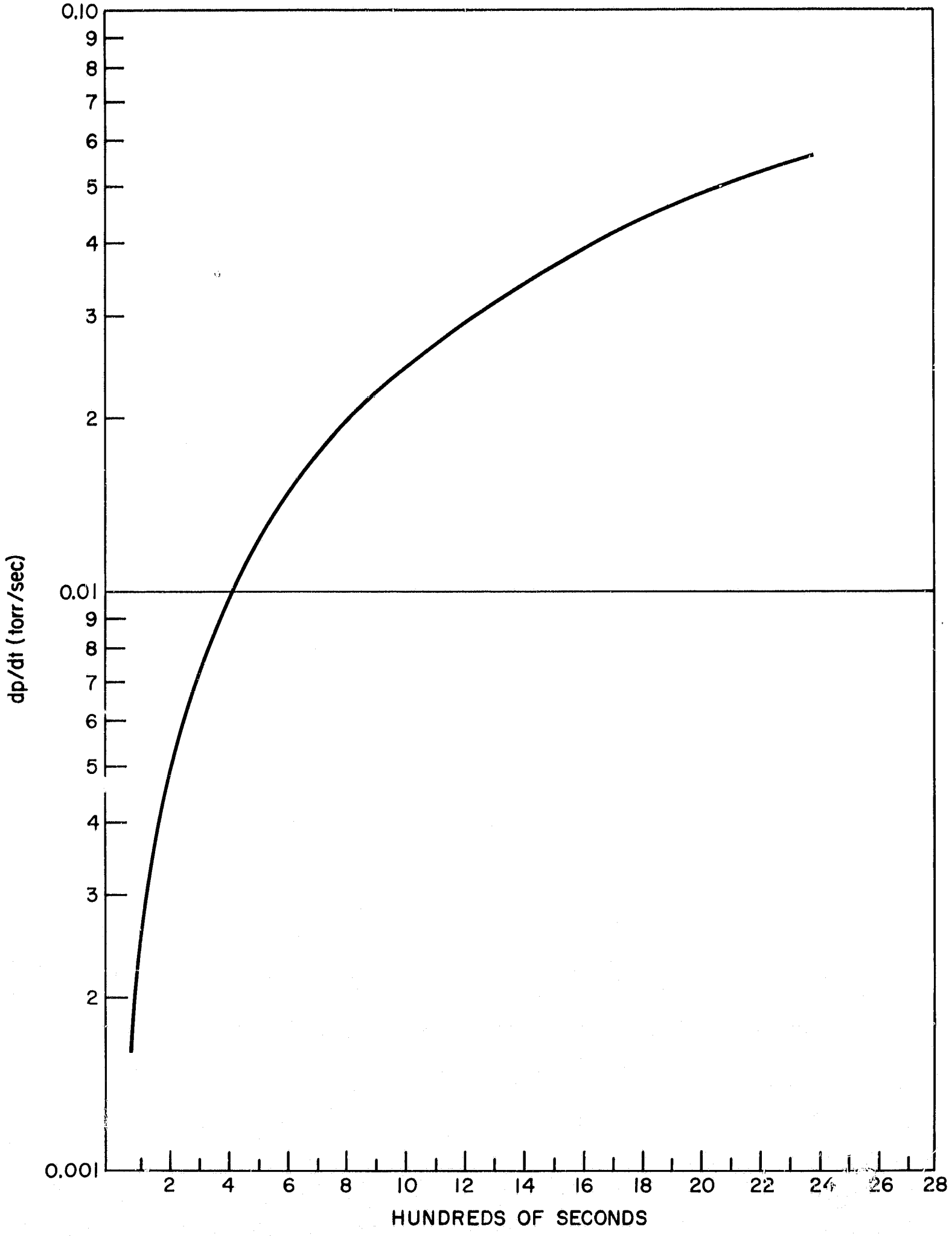

Figure 7. Expected rate of change of ambient pressure vs descent time.

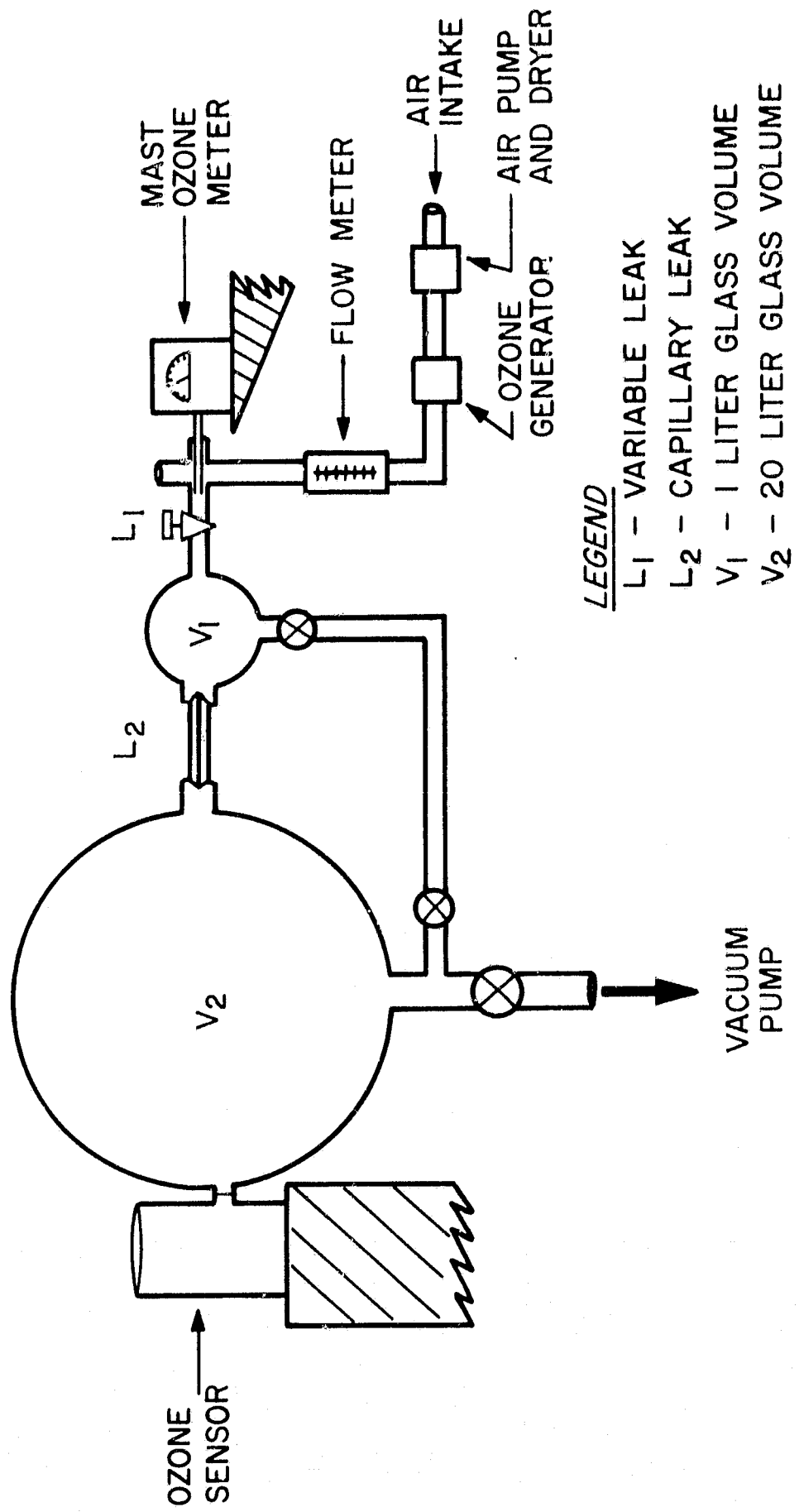

Figure 8. Ozone sensor calibrator.

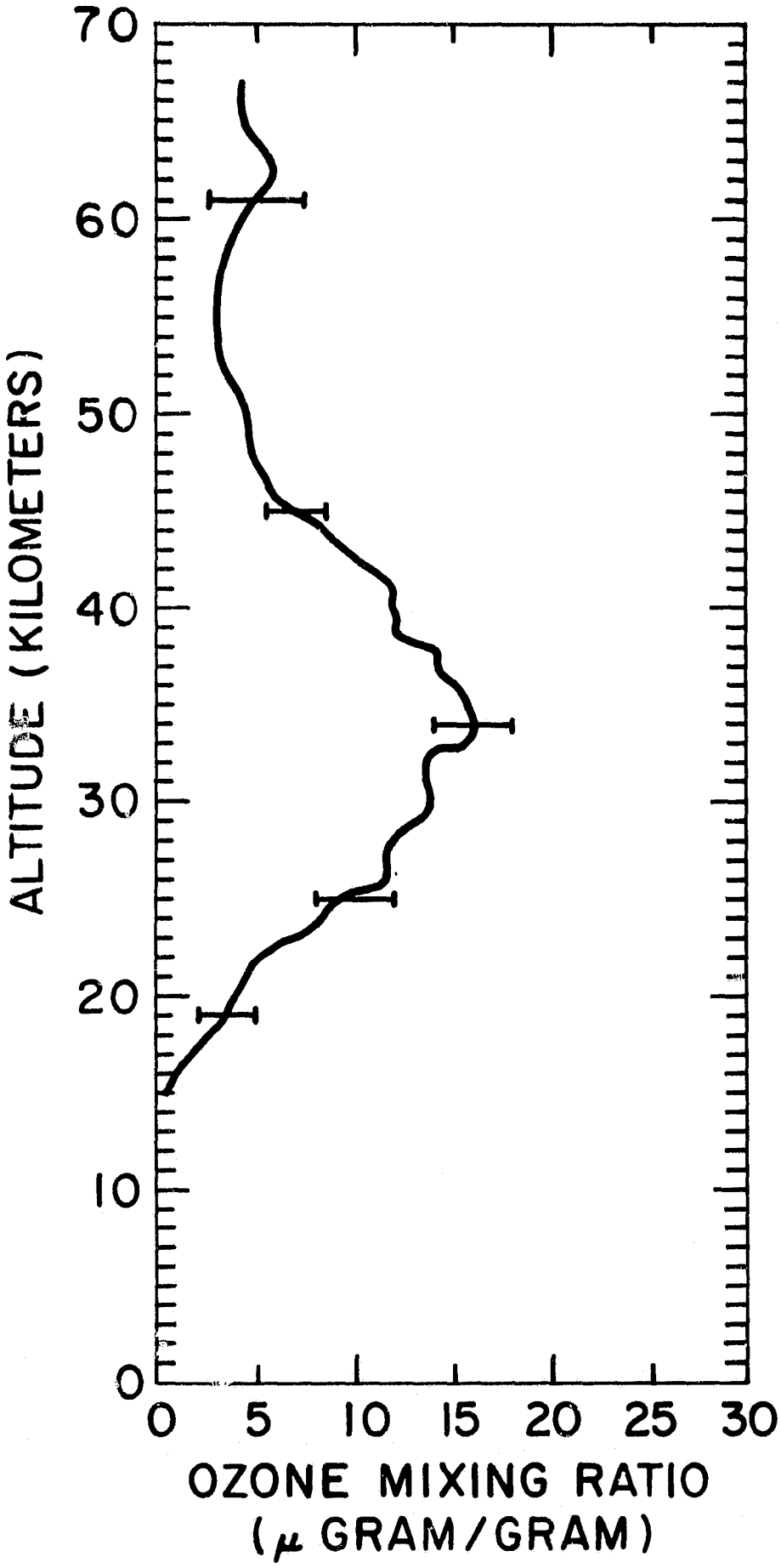

Figure 9. Ozone mixing ratio profile, Wallops Island, Va., September 16, 1968, 1:00 pm EST.

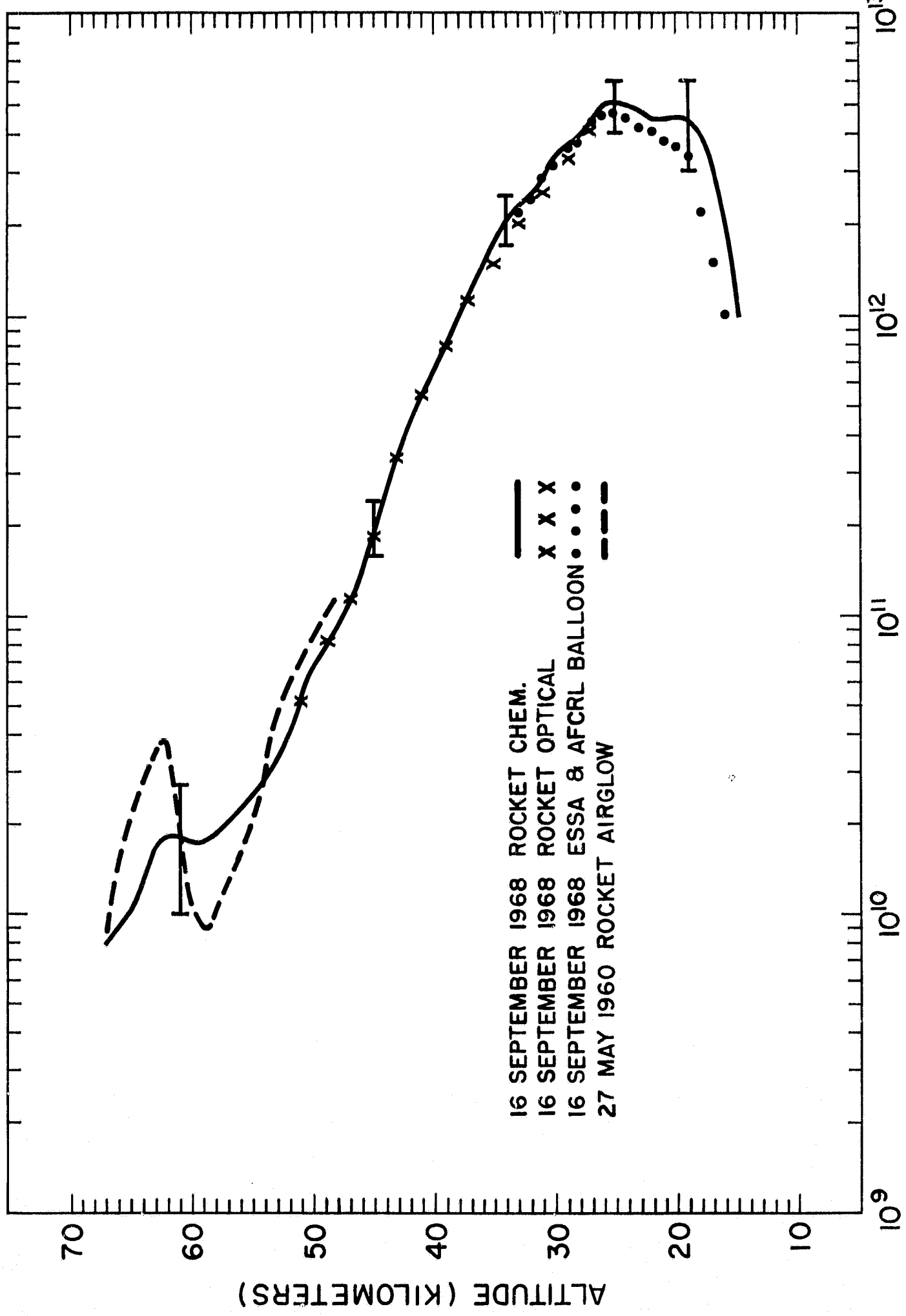

Figure 10. Ozone density profile, Wallops Island, Va., September 16, 1968, 1:00 pm EST.